Nadiah et al (2026)
Vol 14(1): 18165
https://doi.org/10.20884/1.api.2026.14.1.18165

Acta Pharmaciae Indonesia:
Acta Pharm Indo
E-ISSN 2621-4520

RESEARCH ARTICLE Open Access

LC–MS/MS profiling, network pharmacology, and hERG liability docking of *Haliclona* caerulea metabolites as putative cardioprotective candidates

Syaadatun Nadiah[1*], Ahmad Bayu Satriawan[1], Naura Nurnahari[1], Novriadi[2]
[1]Department of Pharmacy, Faculty of Science, Institut Teknologi Sumatera, South Lampung 35365, Lampung, Indonesia
[2]Department of Biology, Faculty of Science, Institut Teknologi Sumatera, South Lampung 35365, Lampung, Indonesia
*Corresponding author: Syaadatun Nadiah, Jl. Terusan Ryacudu, Way Huwi, Jati Agung, South Lampung 35365, Lampung, Indonesia.
E-mail: syaadatun.nadiah@fa.itera.ac.id

ABSTRACT

Introduction: Cardiovascular disease is a leading cause of death worldwide; post-infarction injury involves oxidative stress and inflammation. Cardioprotective leads from marine sponges need early screening for cardiac ion-channel liability, because block of the human ether-à-go-go-related gene (hERG) channel prolongs the QT interval and may provoke fatal arrhythmia. For Indonesian *Haliclona caerulea*, neither the metabolite profile nor its cardiac target space has been reported.

Objectives: To profile metabolites of the n-hexane fraction of *H. caerulea*, predict their myocardial infarction targets, and screen them for hERG liability as a safety filter, not a therapeutic target.

Methods: The fraction was analyzed by untargeted LC–MS/MS and metabolites putatively annotated. Drug-likeness and toxicity were predicted with MolSoft, SwissADME, and ADMETlab 3.0. Candidates were docked into the hERG pore (PDB 8ZYP), benchmarked by re-docking E-4031. Targets came from SwissTargetPrediction, TargetNet, and SEA; disease genes from GeneCards.

Results: All seven metabolites met drug-likeness criteria and returned low ligand-based probabilities (< 0.7) for hERG inhibition, mutagenicity, and carcinogenicity. Docking nevertheless placed neopetrocyclamine A (–11.03 kcal/mol) and adociasulfate 6 (–10.04 kcal/mol) at the E-4031 site with affinities exceeding the blocker, contradicting that result. Network analysis identified 132 shared and ten hub genes.

Conclusion: The target network supports putative cardioprotective interest, whereas docking flags the two strongest pore binders as carrying an unresolved proarrhythmic liability requiring experimental validation.

Keywords: marine natural products, myocardial infarction, proarrhythmic risk, QT prolongation, target prediction

Introduction

Cardiovascular disease remains the leading cause of death worldwide and represents a major challenge in pharmaceutical and biomedical research. Its pathological mechanisms involve oxidative stress, chronic inflammation, and endothelial dysfunction, which together promote atherosclerosis and impair blood flow [1]. Excessive generation of reactive oxygen species (ROS), together with an imbalance of endogenous antioxidant defenses, plays a crucial role in cardiac and vascular cell injury. The development of antioxidant-based cardioprotective agents has therefore become a central focus of pharmacological research [2].

The exploration of natural sources for potential cardioprotective compounds has increasingly shifted toward marine organisms, which are known to produce

Received: October 22, 2025; Revised: October 21, 2026
Accepted: October 22, 2026; Published: October 23, 2026

Copyright © The Author(s) 2026. This article is distributed under a Creative Commons Attribution 4.0 International License

structurally complex secondary metabolites with diverse biological activities. Among these, the blue sponge (*Haliclona caerulea*), commonly found in tropical waters including those of Indonesia, has attracted considerable attention. This species produces a variety of secondary metabolites (steroids, terpenoids, alkaloids, peptides, and unsaturated fatty acids) that exhibit unique chemical structures and broad pharmacological activities [3], including antioxidant, anti-inflammatory, antibacterial, and cytotoxic activities [4,5]. These characteristics make *H. caerulea* a promising candidate for the discovery of novel compounds that may contribute to the treatment of degenerative diseases, including cardiovascular disorders.

Advances in analytical and computational technologies have created new opportunities to identify and evaluate the pharmacological potential of natural compounds more efficiently. Liquid chromatography–tandem mass spectrometry (LC–MS/MS) is a reliable method for profiling bioactive metabolites, and in silico approaches such as molecular docking and network pharmacology are then used to predict compound–protein interactions and to map the biological pathways that may underlie a cardioprotective effect. One molecular checkpoint that every cardiovascular drug candidate must clear is the human ether-à-go-go-related gene (hERG) potassium channel, which conducts the rapid delayed rectifier current (IKr) and governs repolarization of the ventricular action potential. hERG is not a conventional therapeutic target: unintended block of this channel prolongs the QT interval and is the principal mechanism of drug-induced torsades de pointes, which is why regulatory cardiac safety assessment places hERG screening at the front of the development pipeline[6]. In silico hERG screening is therefore used as an early liability filter, and its output requires confirmation by electrophysiological assay [7].

Despite this interest, the metabolite profile of Indonesian *H. caerulea* has not been reported, and no study has mapped its constituents onto the molecular target space of myocardial infarction or examined whether those constituents carry hERG liability. Previous in silico work on marine sponges has generally stopped at binding affinity for a single protein, and has at times treated hERG as a therapeutic target, which conflates efficacy with safety. This study therefore addresses three questions: (i) which metabolites are present in the n-hexane fraction of *H. caerulea*; (ii) which myocardial infarction-related genes and pathways those metabolites are predicted to engage; and (iii) whether any of them is predicted to occupy the hERG pore and thus carry a proarrhythmic liability. We hypothesized that the fraction contains metabolites whose predicted targets converge on the inflammatory, redox, and matrix-remodeling pathways of myocardial injury, and that combining structure-based docking with ligand-based prediction would separate candidates with an acceptable liability profile from those requiring experimental de-risking. To address these questions we applied an untargeted LC–MS/MS approach combined with in silico target prediction, network pharmacology, and molecular docking against the hERG channel as a cardiac safety filter. The expected outcome is a prioritized, safety-annotated candidate list that can guide subsequent in vitro work, together with an explicit statement of which predictions are least certain. All findings reported here are computational and do not by themselves demonstrate cardioprotective activity.

Methods

Research design

This study employed an exploratory and integrative research design that combined analytical chemistry and computational pharmacology approaches. The workflow consisted of four major stages: (1) untargeted metabolite profiling using LC–MS/MS with putative annotation, (2) drug-likeness, pharmacokinetic, and toxicity screening, (3) target prediction and network pharmacology analysis of genes related to myocardial infarction, and (4) molecular docking against the hERG channel as a cardiac safety (liability) filter. Software and database selection followed current in silico natural product workflows [8,9].

Sample

The sample was the n-hexane fraction of the blue sponge (*H. caerulea*). Its constituent metabolites were annotated from the LC–MS/MS data as described below.

LC–MS/MS analysis

High-resolution mass spectrometry analysis was conducted using an ultra-performance liquid chromatography (UPLC) system (ACQUITY UPLC H-Class, Waters, USA) coupled to a quadrupole time-of-flight (QToF) mass spectrometer (Xevo G2-S QToF, Waters, USA). The chromatographic separation was achieved on a C18 column (1.8 µm, 2.1 × 100 mm,

ACQUITY UPLC HSS, Waters, USA) maintained at 50 °C, with the autosampler held at 25 °C. The sample was prepared and injected once; no analytical replicate was performed, and the resulting absence of an estimate of technical variability is acknowledged under limitations of the study.

The mobile phase consisted of solvent A (water containing 5 mM ammonium formate) and solvent B (acetonitrile containing 0,05% formic acid). The analysis was performed using a step gradient elution with flow rate of 0.2 mL/min for 23 minutes. The injection volume was 5 µL, and all samples were pre-filtered through a 0.2 µm syringe filter to remove particulates before analysis.

Mass spectrometric detection was carried out using electrospray ionization (ESI) in positive ion mode, covering a mass-to-charge (m/z) range of 50–1200. The ion source and desolvation parameters were optimized as follows: capillary voltage 3.0 kV, cone voltage 30 V, source temperature 120 °C, desolvation temperature 350 °C, desolvation gas (N2) flow 800 L/h, and cone gas flow 50 L/h. MS/MS spectra were acquired in data-dependent mode with a collision energy ramp of 20–40 eV, and leucine enkephalin was infused as the lock-mass reference for accurate-mass correction. These settings were selected to ensure maximum ionization efficiency and spectral accuracy.

Identification of compounds

The n-hexane fraction of the blue sponge (H. caerulea) was analyzed by liquid chromatography–tandem mass spectrometry (LC–MS/MS) to determine its secondary metabolite profile. The resulting mass spectra were compared with data from the PubChem database and previously reported marine natural product literature to assess the similarity of fragmentation patterns characteristic of the genus Haliclona. Annotation was performed without authentic reference standards; accordingly, all metabolites are reported as putative annotations corresponding to confidence level 2–3 of the Schymanski scale (probable structure by library or literature spectral match, or tentative candidate), and not as confirmed identifications [9]. The acceptance criteria were a mass accuracy within ±5 ppm of the theoretical monoisotopic $[M+H]^+$ ion, an isotope pattern consistent with the proposed molecular formula, and at least two product ions matching literature or in silico fragmentation reported for the genus. Confirmation at level 1 would require co-elution and spectral matching with authentic standards, which were not commercially available for these metabolites. LC–MS/MS was selected for this purpose because it provides high sensitivity and precise molecular characterization of natural products.

Target prediction and network pharmacology analysis

Compounds that passed the screening stage were further analyzed through a network pharmacology approach to predict potential gene targets relevant to myocardial infarction. Target prediction was performed using SwissTargetPrediction [10], TargetNet, and the SEA (Similarity Ensemble Approach), restricted to Homo sapiens. Targets were retained when the SwissTargetPrediction probability was $\geqslant 0.1$ (15 highest-ranked targets per compound), the TargetNet probability was $\geqslant 0.5$, and the SEA E-value was $\leqslant 1 \times 10^{-5}$. The predicted gene datasets from the three tools were merged and de-duplicated by official HGNC gene symbol to generate a non-redundant list of metabolite-associated genes.

Disease-related genes were obtained from the GeneCards database using the keyword “myocardial infarction”, and only genes with a relevance score $\geqslant$ 55 were retained; this cut-off was applied consistently throughout the study. The intersection between metabolite-associated genes and disease-related genes was analyzed using Venny 2.1. Protein–protein interaction (PPI) analysis was conducted using the STRING database (v12.0, Homo sapiens, minimum required interaction score 0.4, disconnected nodes hidden) [11] to identify hub genes, which were ranked by degree centrality.

Network interpretation and validation

The ten genes with the highest degree centrality were designated hub genes. To move beyond a descriptive gene list, hub genes were grouped into functional modules and interpreted in terms of their established roles in myocardial injury and repair, in line with current network pharmacology practice. No enrichment or network result was experimentally validated in this study.

Protein target selection

The hERG potassium channel was used as a cardiac safety target rather than as a therapeutic target. Its

structure was retrieved from the Protein Data Bank (PDB ID 8ZYP), solved in complex with the reference blocker E-4031. The protein structure was downloaded from the Protein Data Bank (https://www.rcsb.org/). The channel is a homotetramer (A4) of *Homo sapiens* with no reported mutations, and the E-4031-bound state defines the canonical pore-blocking site, providing a structural benchmark against which the test compounds can be assessed for pore occupancy.

Compound optimization

The molecular structures of the selected compounds were retrieved from the PubChem database (https://pubchem.ncbi.nlm.nih.gov/) as SMILES strings. The 2D structures were converted into 3D conformations using MolView (MolView.org). Each structure was energy-minimized using Avogadro software with the MMFF94 force field, applying the Steepest Descent algorithm followed by Conjugate Gradient optimization.

The MMFF94 force field was used for geometry optimization because it provides high accuracy for equilibrium geometries, torsional barriers, and non-bonded interactions, including those of hydrocarbons, heteroatom-containing molecules, and aromatic systems similar to the test compounds[12]. The Steepest Descent algorithm was applied during the initial phase of energy minimization to reduce molecular strain efficiently.

The Conjugate Gradient method was then employed; although slower at the outset, it becomes more efficient as the molecule approaches the minimum-energy configuration. Optimization therefore began with Steepest Descent and continued with Conjugate Gradient until a stable geometry was obtained.

Redocking of macromolecule and native ligand

Docking validation was performed by re-docking the macromolecule 8ZYP with its native ligand E-4031, which acts as an inhibitor in the crystal structure. The grid box dimensions were set to 60 × 60 × 60 Å, with grid center coordinates of 143.247, 153.506, and 132.625 for the x, y, and z axes, respectively. The Genetic Algorithm (GA) parameters were configured as follows: 100 runs, a population size of 150, a medium maximum number of evaluations, and the Lamarckian GA algorithm was selected as the output method. The validation results showed an RMSD value of 1.31 Å and a binding free energy (ΔG) of −9.42 kcal/mol, indicating that the docking protocol was valid and reliable for use in subsequent docking simulations of the test compounds.

Docking of the test compounds

The optimized test compounds were docked into the hERG potassium channel using the same protocol applied in the re-docking validation. The docking conditions were refined by adding polar hydrogen atoms to the protein structure and assigning Kollman charges. No structural modifications were made to the test compounds; both rotatable and non-rotatable compounds remained within a reasonable range. The docking output was interpreted as a measure of predicted pore occupancy, that is, the structural plausibility of hERG block, and not as a measure of functional inhibition: docking cannot distinguish a blocker from a non-blocking binder, nor can it yield an IC50. Compounds placed in the E-4031 site with comparable or stronger affinity were therefore flagged as carrying a potential proarrhythmic liability requiring experimental confirmation. Ligand–protein interactions of the best-scoring poses were rendered as two-dimensional diagrams using BIOVIA Discovery Studio Visualizer; Dassault Systèmes, San Diego, CA, USA).

Drug-likeness and toxicity screening

Drug-likeness was screened with MolSoft and SwissADME [13], retaining compounds with a MolSoft drug-likeness score ⩾ 0.1, no more than one violation of Lipinski's rules, and a predicted oral bioavailability score ⩾ 0.55. Compounds that met these criteria were further subjected to toxicity prediction using ADMETlab 3.0 [8], which included the parameters hERG inhibition (at 10 μM), Ames mutagenicity, and carcinogenicity. Molecules with predicted risk probabilities < 0.7 were provisionally classified as low risk. It should be noted that this ligand-based classifier and the structure-based docking described above interrogate hERG liability by different means. The former relies on statistical similarity to training-set compounds and the latter on geometric fit to the pore, so the two outputs may disagree. Any such discordance is reported explicitly rather than resolved in favor of either method, because resolution requires patch-clamp electrophysiology [7].

Statistical analysis

This study involved no experimental measurement, replicate group, or hypothesis test, and no statistical

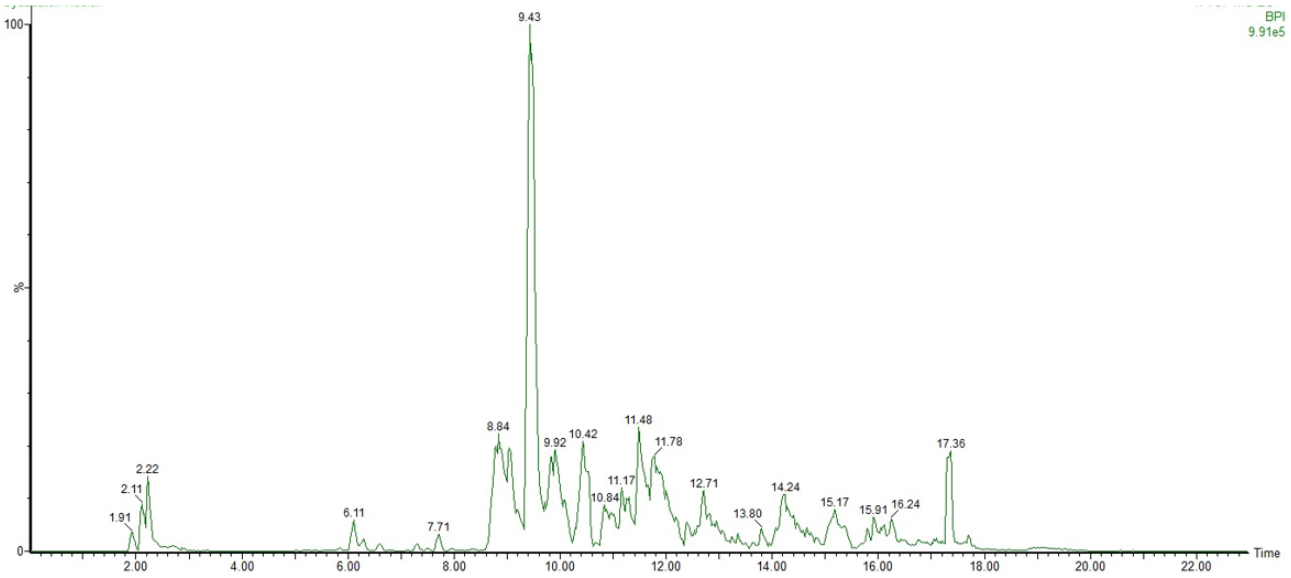


Figure 1. Base peak intensity chromatogram of the n-hexane fraction of *Haliclona caerulea*. Obtained by UPLC–QToF–MS/MS in positive electrospray ionization mode over m/z 50–1200; retention times (min) are shown above the major peaks. UPLC, ultra-performance liquid chromatography; QToF, quadrupole time-of-flight.

analysis was therefore performed. All reported values are single deterministic outputs of the computational tools described above: binding free energies and inhibition constants from AutoDock, probability scores from the ligand-based predictors, and degree-centrality ranks from the protein–protein interaction network. Comparisons between compounds are descriptive, and no measure of dispersion or statistical significance can be attached to them.

Results

Metabolite profiling of the n-hexane fraction

The chromatographic profile of the n-hexane fraction showed several prominent peaks consistent with a complex sponge metabolome (Figure 1). LC–MS/MS analysis putatively annotated seven major metabolites: neopetrocyclamine A (PubChem CID: 122177440), adociasulfate 6 (PubChem CID: 10032033), manzamine A (PubChem CID: 6509753), densanin A (PubChem CID: 171120029), indole-3-carboxylic acid (PubChem CID: 69867), halaminol B (PubChem CID: 10013009), and (1Z,3E)-chlorohexadeca-1,3-diene-5,7-diyne-14-ol, for which no PubChem record is available. Each annotation satisfied the criteria defined in the Methods: the measured accurate mass of the protonated molecule agreed with the theoretical monoisotopic value within ±5 ppm, the isotope pattern was consistent with the proposed molecular formula, and at least two product ions corresponded to fragmentation reported for the genus or predicted in silico. Because authentic reference standards were not available, the annotations remain putative; the full accurate-mass and product-ion data for each metabolite are available from the corresponding author on request. All annotated compounds met the drug-likeness criteria (MolSoft score ⩾ 0.1), did not violate more than one of Lipinski's rules, and showed predicted oral bioavailability scores ⩾ 0.55, suggesting favorable pharmacokinetic characteristics and potential drug-likeness.

Drug-likeness and predicted toxicity

Ligand-based toxicity prediction using ADMETlab 3.0 returned low probabilities (< 0.7) for hERG inhibition, Ames mutagenicity, and carcinogenicity for all seven metabolites, which provisionally classifies them as low risk on these three endpoints.

Target prediction and network analysis

Target prediction using SwissTargetPrediction, TargetNet, and SEA (Similarity Ensemble Approach) yielded 225 non-redundant metabolite-associated genes, of which 132 overlapped with myocardial infarction-related genes (GeneCards relevance score ⩾ 55; Figure 2). Protein–protein interaction (PPI) analysis in STRING identified ten hub genes by degree centrality: PTGS2, ESR1, PARP1, ICAM1, MMP2, GSK3B, JUN, RELA, NR3C1, and SIRT1 (Figure 3).

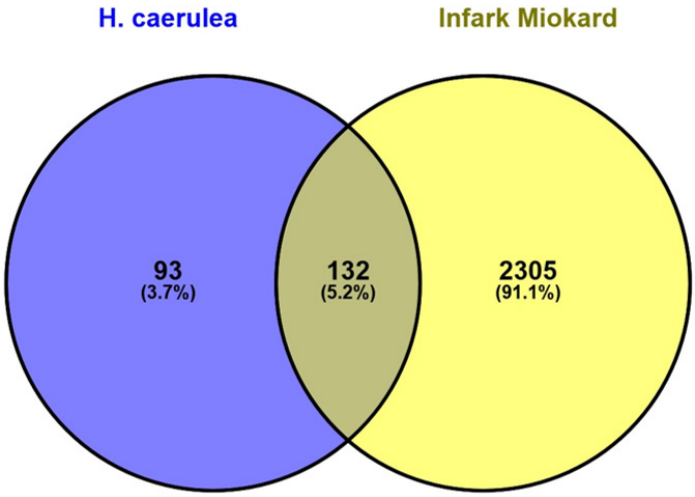


Figure 2. Venn diagram of the overlap between predicted metabolite targets and myocardial infarction-related genes. Metabolite targets (225 genes) were predicted with SwissTargetPrediction, TargetNet, and SEA; disease genes (2,437) were retrieved from GeneCards at a relevance score ≥ 55, and the intersection (132 genes) was computed in Venny 2.1. SEA, Similarity Ensemble Approach.

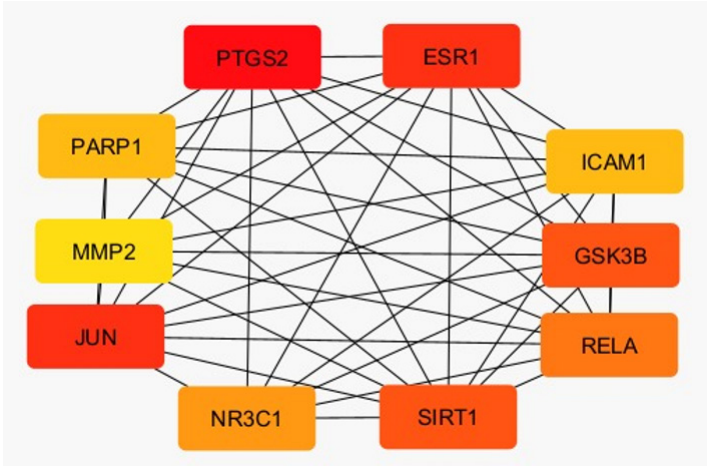


Figure 3. Protein–protein interaction network of the ten hub genes. Constructed in STRING (*Homo sapiens*, minimum interaction score 0.4) from the 132 shared genes and ranked by degree centrality; node color indicates degree, with red the highest.

Validation of the docking protocol

The re-docking validation between the protein structure and its native inhibitor E-4031 produced reliable results, with a root mean square deviation (RMSD) of 1.31 Å and a binding free energy (ΔG) of −9.42 kcal/mol. As illustrated in Figure 4, the overlap between the crystallographic and re-docked conformations of E-4031 showed no significant deviation, with only minor angular shifts observed in flexible regions.

Furthermore, interaction analysis confirmed that these conformational changes did not disrupt key hydrogen bonds or hydrophobic interactions between the ligand and the protein. As shown in Figure 5, hydrogen bonds with Leucine 622 and Serine 649 were preserved, along with additional van der Waals and hydrophobic contacts. With an RMSD below the conventional 2 Å threshold, these results validate the docking protocol and confirm that the same parameters can be applied to the test compounds.

hERG docking of the annotated metabolites

Molecular docking of the seven putatively annotated metabolites into the hERG pore returned the binding free energies summarized in Table 1. All compounds gave negative binding energies, indicating that binding

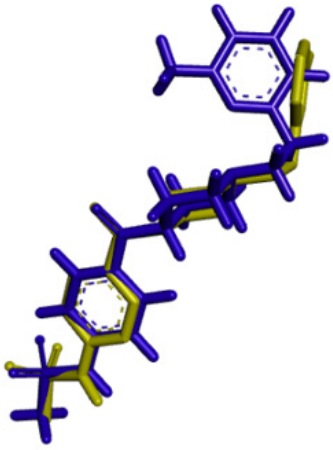


Figure 4. Overlay of E-4031 in the 8ZYP crystal structure (blue) and after re-docking (yellow). Obtained by re-docking the native ligand with AutoDock using the grid parameters described in the Methods, giving a root mean square deviation of 1.31 Å.

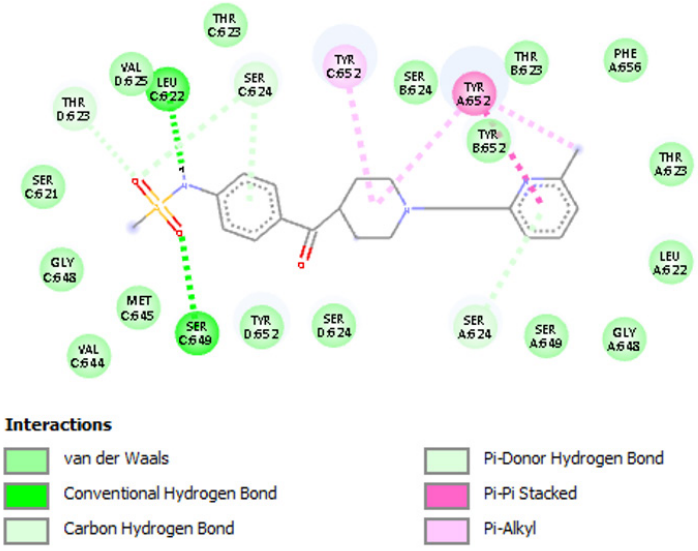


Figure 5. Two-dimensional interaction diagram of the 8ZYP–E-4031 complex after re-docking. Hydrogen bonds and hydrophobic contacts with pore-lining residues are shown; the diagram was generated from the best-scoring docked pose in BIOVIA Discovery Studio Visualizer.

to the pore region is thermodynamically favorable in the model. This is a statement about predicted affinity for the channel which, in the present study, is read as a liability signal rather than as a desirable property.

Neopetrocyclamine A and adociasulfate 6 gave the lowest binding free energies, −11.03 and −10.04 kcal/mol respectively, both exceeding that of the reference blocker E-4031 (−9.42 kcal/mol). Interpreted as a safety screen, this is an unfavorable result: these two metabolites are predicted to occupy the canonical blocker site more avidly than a known IKr blocker, and they are therefore flagged as carrying a potential proarrhythmic liability. This structure-based signal directly contradicts their low ADMETlab hERG probability, and the discordance cannot be resolved with the present data. The remaining five metabolites bound considerably more weakly (−7.38 to −4.67 kcal/mol), concordant with their low predicted liability; on this criterion it is these compounds, rather than the two strongest binders, that present the more acceptable safety profile.

To characterize the binding mode underlying this signal, ligand–protein interactions were visualized and analyzed (Figures 6 and 7).

The binding of E-4031 to the protein typically alters the orientation of key amino acid residues,

Table 1. Predicted binding free energy (ΔG) and inhibition constant (Ki) of the putatively annotated Haliclona caerulea metabolites docked into the hERG channel pore (PDB ID 8ZYP).

No	PubChem CID	Compounds	ΔG (kcal/mol)	Ki (μM)
		Native ligand E-4031	-9.42	0.1252
1	122177440	Neopetrocyclamine A	-11.03	0.00822
2	10032033	Adociasulfate 6	-10.04	0.04386
3	no PubChem record	(1Z,3E)-Chlorohexadeca-1,3-diene-5,7-diyne-14-ol	-7.38	3.89
4	6509753	Manzamine A	-6.78	10.79
5	171120029	Densanin A	-6.7	12.24
6	69867	Indole-3-carboxylic acid	-6.31	23.77
7	10013009	Halaminol B	-4.67	378.15

Values were obtained with AutoDock using the grid parameters validated by re-docking of the reference blocker E-4031. A lower ΔG indicates stronger predicted pore occupancy and therefore a greater predicted proarrhythmic liability. ΔG, binding free energy; Ki, inhibition constant.

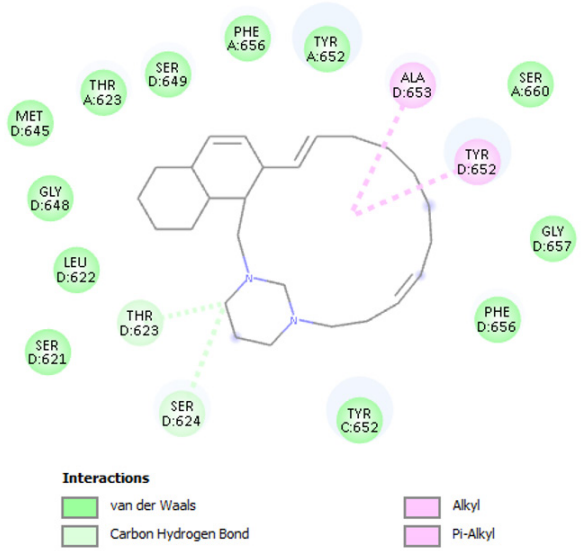


Figure 6. Two-dimensional interaction diagram of neopetrocyclamine A docked into the hERG pore. Hydrogen bonds with Thr623 and Ser624 and a van der Waals contact with Ser649 are shown; the diagram was generated from the best-scoring docked pose in BIOVIA Discovery Studio Visualizer.

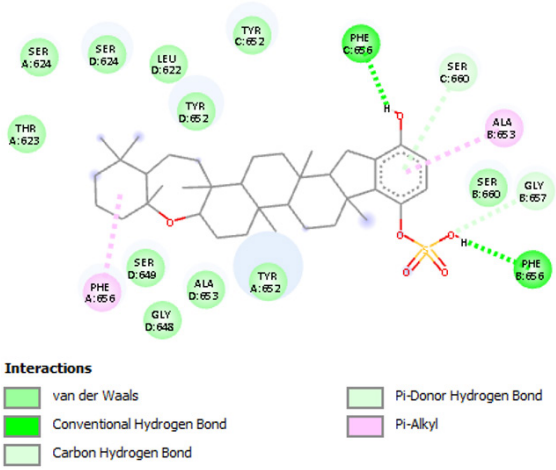


Figure 7. Two-dimensional interaction diagram of adociasulfate 6 docked into the hERG pore. Predominantly van der Waals contacts with Thr623, Ser624, and Ser649 are shown; the diagram was generated from the best-scoring docked pose in BIOVIA Discovery Studio Visualizer.

disrupting the natural symmetry of the channel. This conformational rearrangement indicates that ligand binding can modulate channel function[14]. Following this model, interaction analysis demonstrated that neopetrocyclamine A formed hydrogen bonds with Threonine 623 and Serine 624 and van der Waals contacts with Serine 649. Adociasulfate 6 interacted with Threonine 623, Serine 624, and Serine 649, primarily through van der Waals forces. These residues line the inner cavity of the pore and are the same contacts that stabilize E-4031.

Discussion

The principal contribution of this study is methodological as much as chemical. By combining untargeted metabolite profiling with target-network prediction and an explicit hERG liability screen, it shows that the two most avid pore binders among the metabolites of *H. caerulea* are also the two that carry the clearest predicted proarrhythmic risk. That dissociation between target-network coverage and cardiac safety is easily missed when hERG is treated, as it sometimes is in the natural product docking literature, as a therapeutic target rather than as a liability. The significance of the work therefore lies in showing how an early safety filter changes which candidates are worth pursuing, and in providing a first predicted cardiac target space for an Indonesian population of this sponge.

The putative annotation of seven metabolites from *H. caerulea* illustrates the chemical diversity of marine-derived natural products. Sponges of the genus *Haliclona* have previously been reported to produce structurally complex metabolites such as alkaloids, terpenoids, and peptides, with notable antioxidant, anti-inflammatory, and cytoprotective activities. These findings identify *H. caerulea* as a chemically promising starting point for cardioprotective drug discovery, with the caveat that the annotations remain putative and that chemical diversity alone does not establish pharmacological activity.

The hERG potassium channel was examined not as a therapeutic target but as a cardiac safety checkpoint. hERG conducts the rapid delayed rectifier current (IKr) and governs repolarization of the ventricular action potential; pharmacological block of this channel prolongs the QT interval, predisposes to torsades de pointes, and is the most common cause of cardiac safety attrition in drug development [6]. An agent intended to protect the myocardium after infarction must therefore be shown not to block hERG, and this is the sense in which the channel is used throughout the present study.

The 8ZYP structure was selected because its resolution permits precise visualization of ligand binding within the pore, and because it captures the channel in the blocked state with E-4031 bound. This provides a defined structural reference: a test compound that occupies the same site with comparable geometry and affinity is structurally capable of producing the same block. The structure is therefore used to benchmark liability, not to model a therapeutic interaction.

This endpoint matters because hERG block prolongs ventricular repolarization and the QT interval, and is the principal mechanism of drug-induced torsades de pointes. It is for this reason that hERG was used in the present study as a safety filter rather than as a therapeutic target.

A low ligand-based probability is not, however, evidence of cardiac safety on its own. As shown below, structure-based docking placed two of these metabolites in the E-4031 pore site with affinities exceeding the reference blocker, which is discordant with the ADMETlab classification. The two approaches are not interchangeable: the classifier generalizes from structurally similar training compounds and is therefore least reliable for scaffolds that are poorly represented in its training set, such as polycyclic marine alkaloids and sulfated terpenoids, whereas docking scores geometric complementarity and cannot distinguish pore block from non-blocking binding. Neither output is a functional measurement. The compounds are therefore reported here with both predictions side by side, and the discordant cases are treated as unresolved liabilities rather than as safe [7,8].

Rather than enumerating these genes individually, their functional convergence is the more informative result. The ten hub genes map onto three interconnected axes of post-infarction myocardial injury. The first is an NF-κB-driven inflammatory axis comprising RELA, PTGS2, ICAM1, and JUN: RELA is the transactivating subunit of NF-κB, which after ischemia–reperfusion induces PTGS2 (COX-2) and the adhesion molecule ICAM1, driving neutrophil recruitment and extending infarct size, while JUN contributes through AP-1-dependent co-regulation of the same promoters. The second is a redox and survival axis centered on SIRT1,

with GSK3B and PARP1: SIRT1 coordinates AMPK–FOXO3–Nrf2 signaling to upregulate antioxidant enzymes and sustain mitophagy, and its activity is constrained by PARP1, which competes for the same NAD+ pool during oxidative DNA damage, so that PARP1 overactivation lowers SIRT1-dependent protection [15]. The third is a matrix-remodeling axis in which MMP2 degrades the cardiac extracellular matrix and contributes to adverse ventricular remodeling after infarction.

These three axes are not independent. NF-κB-driven inflammation generates the oxidative burden that depletes NAD+ and limits SIRT1 activity, and both inflammation and oxidative stress upregulate MMP2. A compound set predicted to engage nodes across all three axes would therefore be expected to act through multi-pathway modulation rather than through a single dominant target. ESR1 and NR3C1 are included among the hub genes but are interpreted here with caution, because both are promiscuous in ligand-based target prediction and their high connectivity may partly reflect database bias rather than a specific pharmacological interaction.

Comparable network pharmacology studies of traditional and marine-derived compounds have reported similar regulatory patterns; analyses of traditional Chinese medicine (TCM) preparations for myocardial infarction have converged on PI3K/Akt, NF-κB, and apoptosis signaling, with subsequent molecular docking and experimental validation [16]. The present results are consistent with that pattern. It must be emphasized, however, that the pathway assignments reported here are predictions derived from database annotation and interaction scores, and that no enrichment result was experimentally validated in this study.

E-4031 is a known antiarrhythmic agent used for the treatment of atrial and ventricular fibrillation, acting through inhibition of the Ikr (rapid delayed rectifier potassium current) in cardiac cell [6,17]. The crystal structure 8ZYP pre-presents the inhibited form of the hERG channel in complex with E-4031. The drug interacts with several amino acid residues in the channel, forming both hydrogen bonds and hydrophobic interactions that stabilize the inhibitor within the pore.

Key amino acid residues involved in the interaction include Threonine 623, Serine 624, and Serine 649 across multiple chains. These residues are critical for maintaining inhibitor stability. The piperidine core of E-4031, a structural motif common among hERG blockers, carries a positive electrostatic charge that interacts with the negatively charged regions of the hERG channel, thereby obstructing normal potassium ion transport[14].

Neopetrocyclamine A therefore reproduces the binding pattern of the reference blocker E-4031 within the pore. In a safety context this similarity is the concerning finding rather than a favorable one, because recapitulating the pharmacophore of a known IKr blocker is the structural prerequisite for QT prolongation. Adociasulfate 6, although it does not reproduce the same hydrogen-bond network, still occupies the cavity with a binding energy below that of E-4031. Both compounds consequently require electrophysiological assessment before any further development, whereas the weaker-binding metabolites may be advanced on the basis of a concordant low-liability prediction.

Taken together, these results separate the chemical interest of *H. caerulea* metabolites from their suitability as cardioprotective leads. The network pharmacology analysis indicates that the fraction engages inflammatory, redox, and matrix-remodeling nodes relevant to myocardial infarction, and this is the basis of the putative cardioprotective hypothesis. The hERG docking, by contrast, indicates that the two most avid pore binders in the set carry an unresolved proarrhythmic liability. Candidate prioritization should therefore follow the combination of predicted network coverage and concordant low hERG liability, rather than binding affinity for the channel.

Several constraints should be considered when interpreting these findings. The study is entirely computational: no cellular, electrophysiological, or animal experiment was performed, and consequently none of the reported interactions, pathway assignments, or safety classifications constitutes evidence of biological activity. Metabolite annotations are putative (confidence level 2–3) and were made without authentic reference standards, so compound identities remain provisional and no quantitative abundance was determined. The fraction was injected once, so no technical replicate was available and the reproducibility of peak detection could not be assessed. Docking was carried out on a single rigid-receptor conformation and scored with an empirical function, which neglects channel flexibility, explicit solvation, the membrane environment, and state-dependent access to the hERG pore; binding free energies obtained with AutoDock rank poses more

reliably than they reproduce absolute affinities. Target prediction depends on the composition and bias of the underlying chemical and gene databases, and marine natural product scaffolds are under-represented in those training sets, which lowers confidence for precisely the compounds examined here. The GeneCards relevance cut-off and the PPI score threshold are operator-chosen and alter the size of the overlapping gene set. Finally, no pharmacokinetic exposure modeling was performed, so the concentrations at which any predicted interaction might occur *in vivo* remain unknown.

Conclusion

This study profiled the metabolites of the n-hexane fraction of *H. caerulea*, mapped their predicted target network in myocardial infarction, and screened them for hERG liability. Seven putatively annotated metabolites met the drug-likeness criteria, and their predicted targets converged on three axes of post-infarction injury: NF-κB-driven inflammation, SIRT1-dependent redox control, and MMP2-mediated matrix remodeling. These axes, rather than any interaction with hERG, form the predicted basis of a cardioprotective effect. Docking, however, placed neopetrocyclamine A and adociasulfate 6 in the hERG pore more avidly than the reference blocker E-4031, a signal that contradicts their low ligand-based liability and remains unresolved. The practical implication is that the two most avid binders are the least advanceable without electrophysiological de-risking, whereas the five weaker binders cover the same target network at lower predicted risk. All findings are computational and require experimental confirmation, beginning with patch-clamp measurement of hERG current and verification of compound identity against authentic standards.

Acknowledgment

The authors gratefully acknowledge the financial support provided by the Ministry of Higher Education, Science, and Technology of the Republic of Indonesia. This support was essential in facilitating the research activities, from the exploration and analytical stages to the completion of this scientific manuscript.

Funding

Ministry of Higher Education, Science, and Technology of the Republic of Indonesia, contract no 1483af/IT9.2.1/PT.01.03/2025.

Conflict of interest

The authors declare no conflict of interest.

Author contributions

SN: Investigation; Methodology; Writing – original draft; Conceptualization; Supervision, Project administration, Software, and Funding acquisition. ABS: Formal analysis; Investigation. NN: Formal analysis; Visualization. NV: Resources; Investigation. Writing – review & editing was performed by all authors, who have read and approved the final version of the manuscript.

Declaration of generative AI use

No generative AI tool was used in preparing this manuscript.

References

[1] Valaitienė J, Laučytė-Cibulskienė A. Oxidative stress and its biomarkers in cardiovascular diseases. Artery Res. 2024;30: 1–12. https://doi.org/10.1007/s44200-024-00062-8

[2] Zhang Z, Guo J. Deciphering oxidative stress in cardiovascular disease progression: a blueprint for mechanistic understanding and therapeutic innovation. Antioxidants (Basel). 2024;14: 38. https://doi.org/10.3390/antiox14010038

[3] Karimpoor M, Kamrani E, Yousefzadi M, Nazemi M. Antibacterial and antioxidant potential of *Haliclona caerulea* extracts from Tidal Island Larak, Persian Gulf. Modares J Biotechnol. 2018;9: 347–353.

[4] Varijakzhan D, Loh JY, Yap WS, Yusoff K, Seboussi R, Lim SHE, et al. Bioactive compounds from marine sponges: fundamentals and applications. Mar Drugs. 2021;19: 246. https://doi.org/10.3390/md19050246

[5] Mehbub MF, Yang Q, Cheng Y, Franco CMM, Zhang W. Marine sponge-derived natural products: trends and opportunities for the decade of 2011–2020. Front Mar Sci. 2024;11: 1462825. https://doi.org/10.3389/fmars.2024.1462825

[6] Furutani K. Facilitation of hERG activation by its blocker: a mechanism to reduce drug-induced proarrhythmic risk. Int J Mol Sci. 2023;24: 16261. https://doi.org/10.3390/ijms242216261

[7] Olivia Y, Park H, Ariyadi, Qauli AI, Fuadah YN, Marcellinus A, et al. Incorporating inter-individual variability to improve the reliability of predicted outcomes in in silico cardiac safety assessment. Toxicol Appl Pharmacol. 2026;511: 117831. https://doi.org/10.1016/j.taap.2026.117831

[8] Fu L, Shi S, Yi J, Wang N, He Y, Wu Z, et al. ADMETlab 3.0: an updated comprehensive online ADMET prediction platform enhanced with broader coverage, improved performance, API functionality and decision support. Nucleic Acids Res. 2024;52: W422–W431. https://doi.org/10.1093/nar/gkae236

[9] Schymanski EL, Jeon J, Gulde R, Fenner K, Ruff M, Singer HP, et al. Identifying small molecules via high resolution

mass spectrometry: communicating confidence. Environ Sci Technol. 2014;48: 2097–2098. https://doi.org/10.1021/es5002105

[10] Daina A, Michielin O, Zoete V. SwissTargetPrediction: updated data and new features for efficient prediction of protein targets of small molecules. Nucleic Acids Res. 2019;47: W357–W364. https://doi.org/10.1093/nar/gkz382

[11] Szklarczyk D, Kirsch R, Koutrouli M, Nastou K, Mehryary F, Hachilif R, et al. The STRING database in 2023: protein-protein association networks and functional enrichment analyses for any sequenced genome of interest. Nucleic Acids Res. 2023;51: D638–D646. https://doi.org/10.1093/nar/gkac1000

[12] Halgren TA. Merck molecular force field. I. Basis, form, scope, parameterization, and performance of MMFF94. J Comput Chem. 1996;17: 490–519. https://doi.org/10.1002/(SICI)1096-987X(199604)17:5/6<490::AID-JCC1>3.0.CO;2-P

[13] Daina A, Michielin O, Zoete V. SwissADME: a free web tool to evaluate pharmacokinetics, drug-likeness and medicinal chemistry friendliness of small molecules. Sci Rep. 2017;7: 42717. https://doi.org/10.1038/srep42717

[14] Miyashita Y, Moriya T, Kato T, Kawasaki M, Yasuda S, Adachi N, et al. Improved higher resolution cryo-EM structures reveal the binding modes of hERG channel inhibitors. Structure. 2024;32: 1926–1935.e3. https://doi.org/10.1016/j.str.2024.08.021

[15] Xue T, Wang S, Zhu X, Luo J, Zhu R, Li H, et al. Protective mechanisms of sirtuin family in myocardial ischemia-reperfusion injury and translational therapeutic perspectives. Mol Biol Rep. 2026;53: 1. https://doi.org/10.1007/s11033-026-12521-3

[16] Zhang X, Yang L, Feng K, Zhang H, Chen Y, Li W, et al. Shuxuening injection improves myocardial injury after myocardial infarction by regulating macrophage polarization via the TLR4/NF-κB and PI3K/Akt signaling pathways. Phytomedicine. 2025;138: 156418. https://doi.org/10.1016/j.phymed.2025.156418

[17] Helliwell MV, Zhang Y, El Harchi A, Dempsey CE, Hancox JC. Inhibition of the hERG potassium channel by a methanesulphonate-free E-4031 analogue. Pharmaceuticals (Basel). 2023;16: 1204. https://doi.org/10.3390/ph16091204